Proceedings of the Joint North America, Asia-Pacific ISTVS Conference and Annual Meeting of Japanese Society for Terramechanics

Fairbanks, Alaska, USA, June 23-26, 2007

Modeling of Moguls on an Endurance Test Course

Mark J. Brudnak, Ph.D.

U.S. Army RDECOM-TARDEC, mark.brudnak@us.army.mil

David D. Gunter

U.S. Army RDECOM-TARDEC, dave.gunter@us.army.mil

Wesley Bylsma

U.S. Army RDECOM-TARDEC, wesley.bylsma@us.army.mil

Abstract. *This paper presents an approach to modeling discrete features on a U.S. Army endurance test course. The features in this case are 39 moguls with heights varying between 0.36 and 0.63 m built into a portion of the course. Because they are enumerable and localized, they do not lend themselves to traditional modeling techniques such as RMS, PSD, IRI, etc. We assume that the mogul has a well defined shape and we evaluate five different approaches to modeling this shape assuming that each mogul may be thought of as an ideal shape superimposed with stationary noise. The models that we evaluate are the Gaussian function, the Hanning window, the support vector machine, a two-Gaussian function and a two-Gaussian function with fixed width and amplitude ratios. We evaluate these models by computing the RMS error of each best fit and by evaluating the stationarity of the residue. We further evaluate each mogul model by running a HMMWV dynamics model over each and comparing several responses to those obtained from the profiled mogul. In our analysis we find that a model consisting of two Gaussian functions with related widths and amplitudes yields an unbiased estimate of a mogul and can be made to approximate any mogul by adjusting its width and amplitude.*

Keywords. Terrain profile, mogul, model, curve fitting, Gaussian, SVM, Hanning window, HMMWV.

1 Introduction

The U.S. Army performs endurance testing of its vehicles at several proving grounds each of which have various courses to represent primary, secondary and cross-country terrains. These courses are used by the Army to evaluate vehicles against contractual reliability requirements. It is, therefore, in the interest of both the Army and its vehicle developers to measure, characterize, and understand the essential features of these courses. Such an understanding helps the Army monitor and maintain course severity and helps the contractor know how its vehicle will be evaluated. All terrain monitoring begins with a measurement of the terrain profile, for which there are many available techniques which are nicely summarized by Sayers and Karamihas (1998). A road profile is a measurement of terrain elevation vs. horizontal distance along the course. The horizontal resolution of such profiles varies from 0.3 m to 1 mm; they may have

Report Documentation Page

Form Approved
OMB No. 0704-0188

1. REPORT DATE	2. REPORT TYPE	3. DATES COVERED
23 JUN 2007	**N/A**	**-**

4. TITLE AND SUBTITLE	5a. CONTRACT NUMBER
Modeling of Moguls on an Endurance Test Course	5b. GRANT NUMBER
	5c. PROGRAM ELEMENT NUMBER
6. AUTHOR(S)	5d. PROJECT NUMBER
Brudnak, Mark J, Ph.D.; Gunter, David D; Bylsma, Wesley	5e. TASK NUMBER
	5f. WORK UNIT NUMBER
7. PERFORMING ORGANIZATION NAME(S) AND ADDRESS(ES)	8. PERFORMING ORGANIZATION REPORT NUMBER
USATACOM 6501 E 11 Mile Road Warren, MI 48397-5000	**17031RC**
9. SPONSORING/MONITORING AGENCY NAME(S) AND ADDRESS(ES)	10. SPONSOR/MONITOR'S ACRONYM(S)
	TACOM TARDEC
	11. SPONSOR/MONITOR'S REPORT NUMBER(S)
	17031RC

12. DISTRIBUTION/AVAILABILITY STATEMENT
Approved for public release, distribution unlimited

13. SUPPLEMENTARY NOTES
The original document contains color images.

14. ABSTRACT

15. SUBJECT TERMS
Terrain profile, mogul, model, curve fitting, Gaussian, SVM, Hanning window, HMMWV

16. SECURITY CLASSIFICATION OF:			17. LIMITATION OF ABSTRACT	18. NUMBER OF PAGES	19a. NAME OF RESPONSIBLE PERSON
a. REPORT	b. ABSTRACT	c. THIS PAGE			
unclassified	**unclassified**	**unclassified**	**SAR**	**16**	

lengths varying from 30 m to 10 km (or more) and are typically measured for two vehicle tracks. The volume of information and the random nature of the raw profile data motivates their reduction to some essential features which are preferably invariant to the statistical variation observed in the profile measurement. It is desired that these features correlate to a vehicle performance metric such as ride quality or durability. A one statistic traditionally used by the Army has been the root mean square (RMS) of the detrended terrain profile which works well for terrains which are stationary. It is appealing because it captures the roughness in one number. Recently, the Amy has begun to characterize its profiles with the power spectrum density (PSD) (or more correctly the wave number spectrum). Typically these PSDs are then used to generalize the frequency-domain shape to a sloped line which approximates the PSD. Such representations are usually documented in the form of a frequency-domain plot with labeled slopes and breakpoints. The PSD is again appealing in that it captures the essential terrain information in a few parameters represented in a plot; it however assumes that the terrain profile is statistically stationary (see Steinwolf et al, 2005). The automotive industry has developed their own metrics for road roughness called the International Roughness Index (IRI), and the Speed Roughness Index (SRI). The IRI is a computation based on the cumulative suspension displacement of the so called “Golden car model” run over the profile at a fixed speed. The SRI adjusts the IRI for speed.

Given these characterizing features (e.g. RMS, PSD, IRI), it is often desired to reverse this process; that is, given some roughness metric, synthesize a terrain profile which is a faithful representation of the original terrain profile. In the synthesis problem, it is important that enough features be retained from the original profile to allow proper reconstruction. Single-value metrics such as RMS, IRI, and SRI are not suited to profile synthesis. The PSD feature of a profile has been used by the Army in terrain synthesis, however, the resulting profiles are stationary and have random phase relationships, normally not like the actual profile. Sandu et al (2005) has proposed terrain synthesis based on polynomial chaos. Sandu and Li (2007) recently proposed terrain synthesis based on ARMA and ARIMA models. Sun et al (2005) applied uniform modulated processes (UMP) and empirical mode decomposition (EMD) to the synthesis of non-stationary terrain profiles such as are typically measured at Army proving grounds.

Each of these methods of terrain characterization and synthesis approach the problem in an agnostic manner, treating the terrain profile as a time-series with certain assumed properties (i.e. Gaussian, stationary, correlated, etc). None of them however, address the circumstance in which there is a mix of random and non-random features in a terrain profile. Although this is normally a valid assumption, it is not always the case. The topic of this paper is to present an approach to modeling particular non-random features (moguls) on a particular Army proving ground course for the purposes of both characterization and synthesis. It is the intent of this paper to statistically characterize these moguls using a number of candidate functions and determine which is most suitable. We choose direct metrics based on quality of fit and indirect metrics derived from HMMWV dynamics model traversing the moguls. Functions which are fit to the moguls are Gaussian, Hanning, Support Vector Machines, two summed Gaussians, and to ratio-related Gaussians.

2 Profile Description

The particular course in view is used by the Army for endurance testing and has a particular section containing 39 moguls with heights varying between 0.35 and 0.65 m spaced at approximate 30 m intervals. Figure 1 shows a section of this terrain which attempts to place the

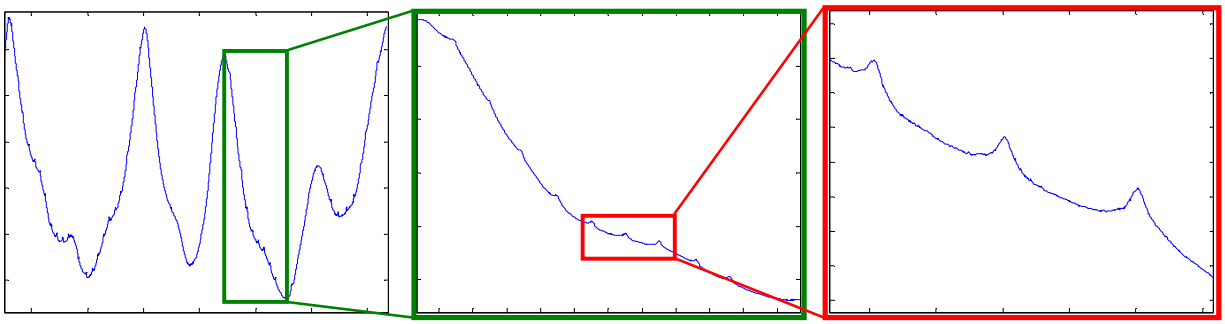

Figure 1. Three plots of the course being analyzed. (left) 2 km section of the course containing the 39 moguls, (middle) view of a single pass of moguls, (right) view of three moguls on a representative grade. The plots are not to scale.

moguls in reference to the entire profile. The profile data used in the following analysis was taken from this course in 2002. The profile consists of correlated right and left track separated by 1.22 m (4 ft) and the longitudinal resolution is 7.62cm (3 in.). The device which measured the profile was developed by the U.S. Army Aberdeen Proving Ground (APG) for the monitoring of course roughness (Castaldo et al, 1991).

3 Modeling Approaches

To begin we note that most of the moguls are situated on graded terrain and since we are interested in modeling the ride and shock aspects of them we will remove the grade information in our analysis. We selected each mogul by finding its center point. Each mogul was extracted from the terrain profile by taking 120 sample points ahead and behind this center point, so each mogul was roughly contained at the center of a 18.28 m (60 ft) stretch of terrain (segment). Each segment was then subjected to a linear least squares analysis and the prevailing bias and slope were removed. A plot of these detrended mogul segments is shown in Figure 2. Next we chose the point in the horizontal axis where we regard the mogul to begin and end. By observing Figure 2 it is clear that the traces of the moguls agree fairly well in the interval [-6m, +6m] and that the agreement between the moguls lessens at distances more than 6 m from the center. We will therefore perform our analysis on an interval of ± 6m (± 20 ft) resulting in an assumed width of 12.2 m (40 ft). It is clear in Figure 2 that the heights of the moguls vary from

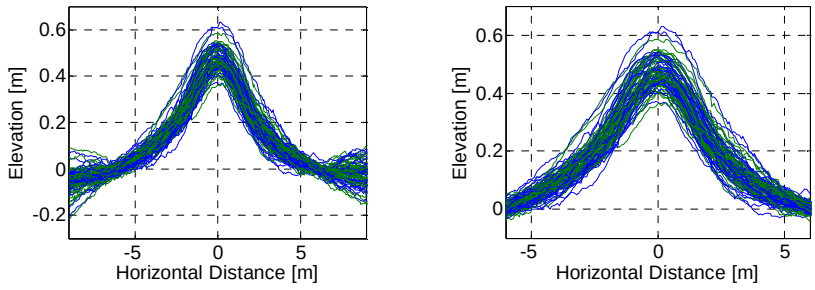

Figure 2. Plot of 39 moguls overlaid. (left) plot over the segment [-9m, 9m]. (right) plot over the horizontal interval [-6m, 6m] for comparison to the fit moguls. Right track traces are in blue and left track traces are in green. Observe that the moguls range in height from 0.36 m to 0.63 m.

approximately 0.36 m to 0.63m and we expect our analysis to show that the widths vary as well.

In our modeling approaches we will seek to minimize the mean squared error (MSE) between the actual mogul data and our model. We will regard each mogul as a set of ordered pairs $\{(x_i, y_i)\}_1^{\ell}$ where x_i is the horizontal distance, y_i is the corresponding elevation and ℓ is the number of samples, which, in our case is 161. Our models will take the continuous form $\hat{y} = f(x;\mathbf{p})$ where x is the independent variable, $\mathbf{p}$ is a vector of parameters to be optimized. We use the "hat" notation to denote an estimated value. Finally we define the particular estimates as $\hat{y}_i = f(x_i;\mathbf{p})$. Our optimization problem will then consist of minimizing the functional

$$\min_{\mathbf{p}}: \quad \sum_{i=1}^{\ell}\left(f(x_i;\mathbf{p}) - y_i\right)^2 + C\mathcal{P}(\mathbf{p}) \tag{1}$$

where $\mathcal{P}(\bullet)$ is a regularization functional and C is a regularization constant (which we will normally choose to be zero). Then by observing Figure 2 we are inclined be believe that the shape of these moguls closely resembles a bell type curve, so our first attempts will be based on the Gaussian function and the Hanning window.

3.1 The single Gaussian function

We will begin our search for the best fit of the mogul by choosing a Gaussian function of the following form

$$f(x;\mathbf{p}) = ae^{\frac{-(x-\bar{x})^2}{2\sigma^2}} + bx + c \tag{2}$$

where the vector of free parameters is $\mathbf{p} = [a \quad \bar{x} \quad \sigma \quad b \quad c]^T$. Although the position $\bar{x}$, bias c and slope b are products of the optimization, they are present to eliminate biased errors due to shifts in the reference data. In this representation, we will take the value a to be the mogul amplitude and since σ is the standard deviation, we will regard the width of the bump as $w = 6\sigma$ (i.e. $\pm 3\sigma$). After optimizing (1) given (2) the fit functions are shown in Figure 3. There it may be observed that the error is biased based on the distance from the center of the mogul. The RMS errors for the right track are on the interval [0.95 cm, 2.58 cm] with an average of 1.63 cm. Likewise, for the left track the RMS error falls in the range [0.79 cm, 2.27 cm] with an average of 1.62 cm. This bias in the error motivates us to look for a better candidate function.

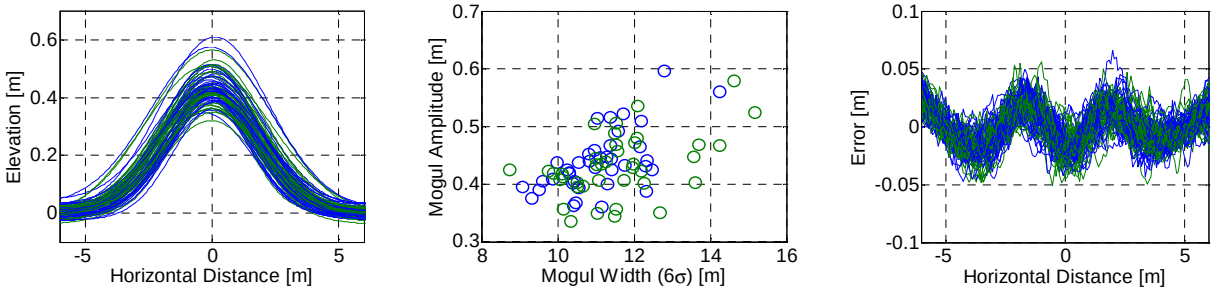

Figure 3. (left) Plot of the Gaussian best fit for the 39 moguls. (middle) Plot of the mogul amplitude (a) vs. the mogul width (6σ). (right) Plot of the error from the Gaussian best fit. Note scales are not the same.

3.2 The Hanning window function

Our next candidate function is the so called Hanning window which has been used on some occasions as a road disturbance input (see Lin et al, 1995). In our case the Hanning function takes the following form

$$f(x;\mathbf{p}) = \begin{cases} \frac{a}{2}\left(1+\cos\left(\frac{2\pi}{w}(x-\bar{x})\right)\right)+bx+c, & -\frac{w}{2} \le x-\bar{x} \le \frac{w}{2} \\ 0, & \text{otherwise} \end{cases} \tag{3}$$

where the vector of free parameters is $\mathbf{p} = [a \quad \bar{x} \quad w \quad b \quad c]^T$. In this representation, we will take the value a to be the mogul amplitude and w as the width. After optimizing (1) given (3) the fit functions are shown in Figure 4. There it may be observed the error is biased based on the distance from the center of the mogul as it was for the Gaussian function. The RMS errors for the right track are on the interval [1.29 cm, 3.18 cm] with an average of 2.33 cm. Likewise, for the left track the RMS error falls in the range [1.33 cm, 3.08 cm] with an average of 2.28 cm. Examining these results with those of the Gaussian best fit it appears that, in general, the Gaussian function is a better representation of the moguls than the Hanning window, we therefore will eliminate the Hanning function from further consideration.

3.3 The Support Vector Machine (SVM) function

Since our analysis thus far has shown that one Gaussian function provides a reasonable fit, we speculate that a set of superimposed Gaussian functions may perform better. We therefore will employ a recently developed technology called Support Vector Machines (SVM) (see Crisianini and Shawe-Taylor (2000) for a full development of the theory) to find a suitable class of functions with which to fit our moguls. The form of the SVM estimator is as follows

$$f(x;\mathbf{p}) = \sum_{i=1}^{\ell} \beta_i e^{-\gamma(x-x_i)^2} + b \tag{4}$$

where the vector of free parameters is $\mathbf{p} = [\beta_1 \quad \beta_2 \quad \cdots \quad \beta_\ell \quad b]^T$ consisting of the weights β_i and the bias b and the values x_i are the horizontal distances from our mogul center. In SVM theory $k(x,y) \triangleq e^{-\gamma(x-y)^2}$ is called the Gaussian *kernel function* for which we are free to choose

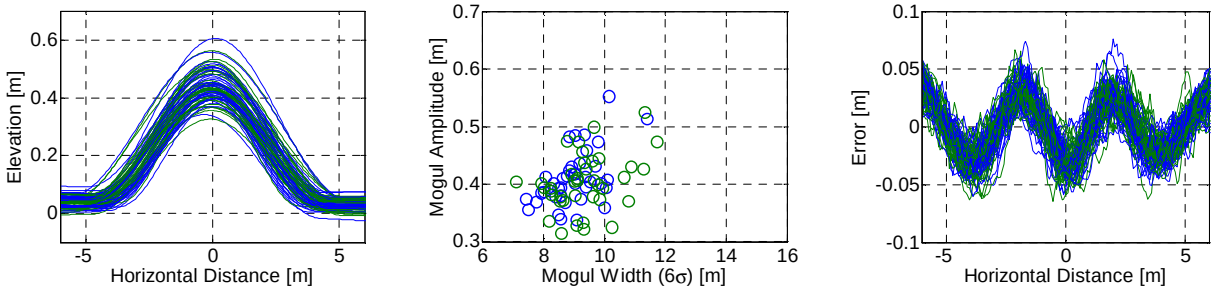

Figure 4. (left) Plot of the Hanning window best fit for the 39 moguls. (middle) Plot of the mogul amplitude (a) vs. the mogul width (w). (right) Plot of the error from the Hanning window best fit. Note scales are not the same.

the kernel parameter γ. The parameters $\mathbf{p}$ are found by solving the following quadratic programming problem

$$\begin{aligned} \min_{\{\beta_i\}}: \quad & \sum_{i=1}^{\ell}\sum_{j=1}^{\ell}\beta_i\beta_j e^{-\gamma\left(x_i-x_j\right)^2} + \sum_{i=1}^{\ell}\beta_i y_i - \varepsilon\sum_{i=1}^{\ell}\left|\beta_i\right| \\ \text{subject to:} \quad & \sum_{i=1}^{\ell}\beta_i = 0, \quad -C \le \beta_i \le C \end{aligned} \tag{5}$$

where ε indicates an upper absolute bound on the error we wish to tolerate and C is a regularization constant. In our analysis we chose $\gamma = 0.149$ 1/m^2 (0.0138 1/ft^2) as the kernel parameter, which corresponds to a width of 10.97 m (36 ft) and was determined by examining the average width generated in the Gaussian fit (Figure 3). We chose the error bound ε to be 2.54 cm (1 inch) and the regularization constant to be 63.5 cm (25 inches). By design, the solution of (5) is sparse in the set of weights $\{\beta_i\}_1^{\ell}$ and those x_i for which $\beta_i \neq 0$ are called *support vectors*. Also the value of the bias b is uniquely determined by the so called KKT conditions and the values of $\{\beta_i\}_1^{\ell}$. In the optimization it was found that the number of support vectors varied from 5 to 16. After optimization of (5) the fit functions are shown in Figure 5. We observe that the error for the most part is unbiased and is mostly clamped at $\pm\varepsilon$, which the SVM algorithm does by design. The RMS errors for the right track are on the interval [1.27 cm, 1.63 cm] with an average of 1.42 cm. Likewise, for the left track the RMS error falls in the range [1.20 cm, 1.65 cm] with an average of 1.42 cm. Comparing these results to both the Gaussian Hanning window approaches, the SVM clearly out performs them both in terms of average RMS error however, the Gaussian function does better for some of the moguls as indicated by the minimum RMS error. The strength of the SVM approach is that by adjusting the parameter ε we can obtain an (almost) arbitrary amount of precision. The weakness of the SVM approach is that it is a black box algorithm that yields no particular insight to the generalized shape of a typical mogul. Since our goal is find a mogul model with two parameters, amplitude and width, we will continue to evaluate other models.

3.4 The Two-Gaussian function

Knowing that the superposition of several Gaussians improves the fit (at least for some moguls) we will next build a hypothesis function composed of two Gaussian functions. These functions

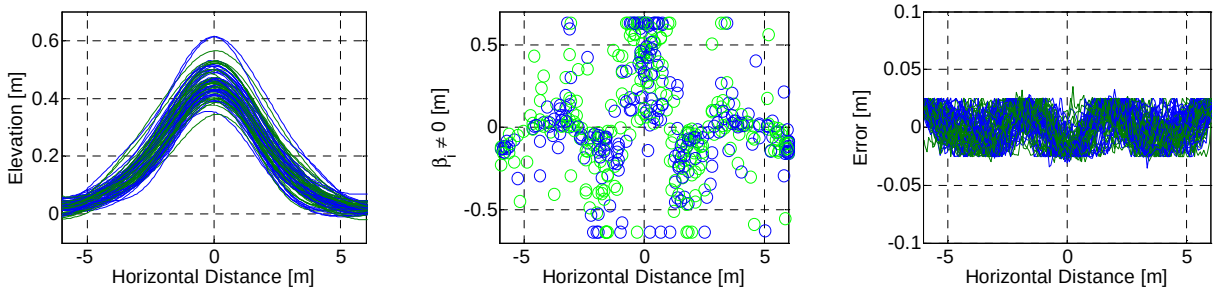

Figure 5. (left) Plot of the SVM best fit for the 39 moguls. (middle) Plot of the weights β_i vs. the support vectors x_i for $\beta_i \neq 0$. (right) Plot of the error from the SVM best fit. Note scales are not the same.

will have freedom to vary independently in amplitude and width, however they will be centered on the same point, $\bar{x}$. Our candidate function takes the following form

$$f(x;\mathbf{p}) = a_1 e^{\frac{-(x-\bar{x})^2}{2\sigma_1^2}} + a_2 e^{\frac{-(x-\bar{x})^2}{2\sigma_2^2}} + bx + c \tag{6}$$

where the vector of free parameters is $\mathbf{p} = [a_1 \quad a_2 \quad \bar{x} \quad \sigma_1 \quad \sigma_2 \quad b \quad c]^T$. (It is worth noting that (6) may be thought of as a 1-2-1 artificial neural network with Gaussian activation functions in the hidden layer and a linear output function.) In this representation, we will take the sum $a_1 + a_2$ to be the mogul amplitude and width we will regard as $w \triangleq 6(a_1\sigma_1 + a_2\sigma_2)/(a_1 + a_2)$ which is a weighted average of the two Gaussian widths. In this case, it was discovered that the optimization problem was ill-posed (see Tikhonov & Arsenin, 1977) and we therefore introduced the regularization functional $\mathcal{P}(\mathbf{p}) \triangleq a_1^2 + a_2^2 + \sigma_1^2 + \sigma_2^2$ and the regularization constant $C = 0.1$ from (1) to stabilize the solution. After optimizing (1) given (6) the fit functions are shown in Figure 6. There it may be observed that the error is for the most part unbiased. The RMS errors for the right track are on the interval [0.57 cm, 2.07 cm] with an average of 1.13 cm. Likewise, for the left track the RMS error falls in the range [0.58 cm, 2.03 cm] with an average of 1.06 cm. Examining these results with those of the prior models it appears that the superposition of two independent Gaussian functions provides the best fit thus far. It is encouraging to see that the addition of the second function is able to effectively compensate for the positional bias found in the single Gaussian approach. In this case we currently have doubled the number of significant parameters from two to four. We may now ask if the parameters a_1, a_2, σ_1, and σ_2 are truly independent. Shown in Figure 7 are two plots which will help answer this question. The left plot shows the width and amplitudes of both Gaussians independently which after training the wider/taller Gaussians were labeled with a_1 and σ_1 while the narrower/shorter ones were labeled with a_2 and σ_2. In this plot we observe that the first and second Gaussian parameter sets tend to cluster into two groups indicating that there may be a relationship between the parameters which we will hypothesize to be proportional. To test this hypothesis we compute the ratios of widths (i.e. σ_2/σ_1) and amplitudes (i.e. a_2/a_1) for all 39 moguls. These ratios are plotted in Figure 7 on the right. Furthermore we compute the average value of each of these ratios to obtain the desired proportional relationships as $p_\sigma \triangleq \overline{\sigma_2/\sigma_1} = 0.431$ and $p_a \triangleq \overline{a_2/a_1} = 0.551$. Our next and last set of functions to evaluate will

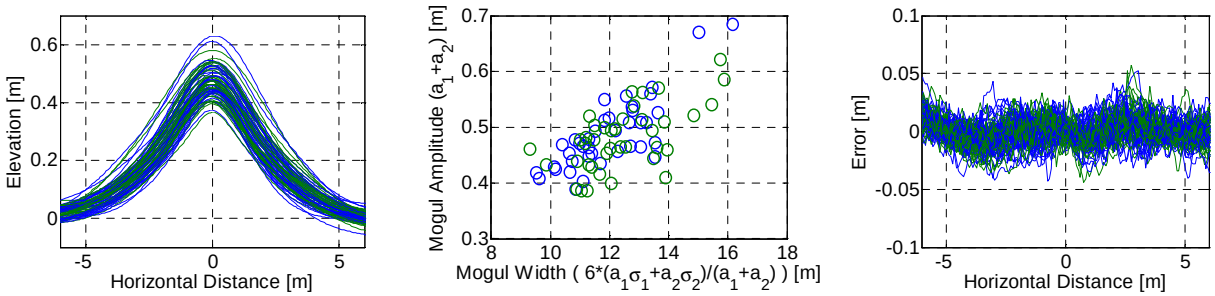

Figure 6. (left) Plot of the two-Gaussian best fit for the 39 moguls. (middle) Plot of the mogul amplitude vs. width as estimated. (right) Plot of the error from the two-Gaussian best fit. Note scales are not the same.

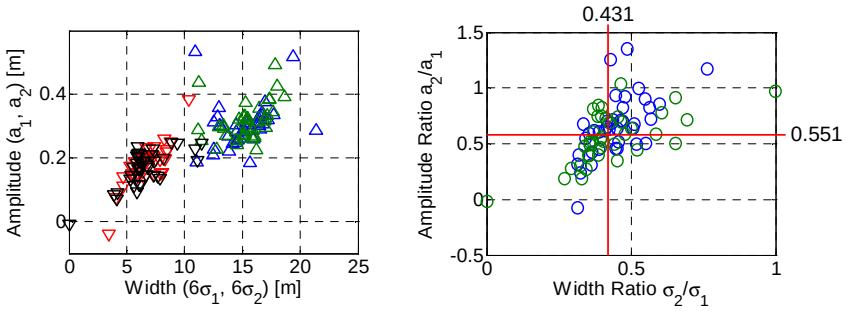

Figure 7. Plot of the parameter relationships for the two-Gaussian best fit for the 39 moguls. (left) The raw parameters. The △ symbol represents $6\sigma_1$ vs. a_1 (red = right, black = left) and the ▽ symbol represents $6\sigma_2$ vs. a_2 (blue=right, green=left). (right) The parameter ratios a_2/a_1 vs. σ_2/σ_1. The red lines represent the average value for each of these ratios.

consist of two Gaussians with widths and amplitudes related by these ratios.

3.5 The Fixed-Ratio Two-Gaussian Function

Knowing that the superposition of two independent Gaussians improves the fit and that the parameters appear to be proportionally related, we will next build a hypothesis function composed of two Gaussian functions based on these ratios. This function will have freedom to vary in amplitude and width only. The widths and amplitudes of the superimposed Gaussians will then be derived from these meta-parameters. In our construction we will always assume that $\sigma_1 > \sigma_2$ and $a_1 > a_2$ and we desire that the width be defined as $w = 6\sigma_1$ and the amplitude $a = a_1 + a_2$. Taking these relations along with the ratios $p_\sigma \triangleq \sigma_2/\sigma_1$ and $p_a \triangleq a_2/a_1$ we derive the Gaussian parameters from w and a as follows:

$$\sigma_1 = \frac{w}{6} \quad \text{(a)} \qquad \sigma_2 = \frac{p_\sigma w}{6} \quad \text{(b)}$$
$$a_1 = \frac{a}{1+p_a} \quad \text{(c)} \qquad a_2 = \frac{a}{1+1/p_a} \quad \text{(d)} \tag{7}$$

where, again, we define $p_\sigma = 0.431$ and $p_a = 0.551$. Our function then is constrained by the relations in (7) and takes the form

$$f(x;\mathbf{p}) = a_1 e^{\frac{-(x-\bar{x})^2}{2\sigma_1^2}} + a_2 e^{\frac{-(x-\bar{x})^2}{2\sigma_2^2}} + bx + c \tag{8}$$

where the vector of free parameters is now $\mathbf{p} = \begin{bmatrix} a & \bar{x} & w & b & c \end{bmatrix}^T$. Because of the constraints in (7) the optimization problem is once again well-posed and we will therefore set the regularization parameter C to zero. After optimizing (1) given (7) and (8) the fit functions are shown in Figure 8. There it may be observed that the error is for the most part unbiased based on the distance from the center of the mogul. The RMS errors for the right track are on the interval [0.65 cm, 2.13 cm] with an average of 1.24 cm. Likewise, for the left track the RMS error falls in the range [0.57 cm, 2.08 cm] with an average of 1.19 cm. Although the

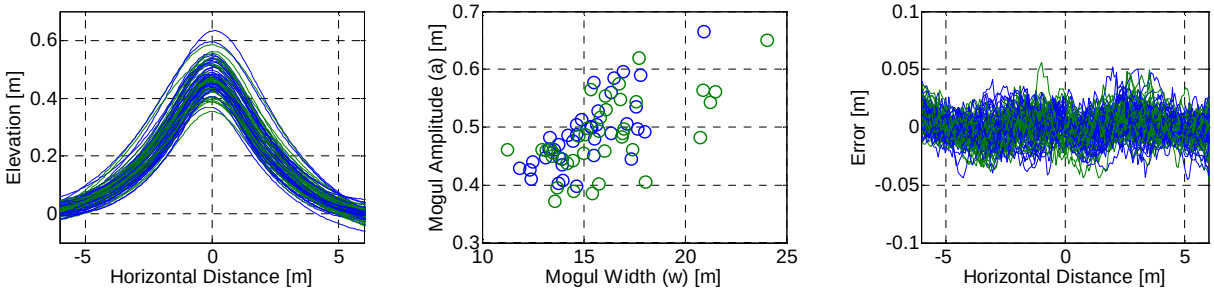

Figure 8. (left) Plot of the ratio-Gaussian best fit for the 39 moguls. (middle) Plot of the mogul amplitude vs. width as estimated. (right) Plot of the error from the two-Gaussian best fit. Note scales are not the same.

performance is very slightly worse than the independent two-Gaussian fit this model is appealing because its shape is fixed and the tunable parameters are intuitive.

3.6 Mogul Model Comparisons

Now that we have computed the results of the five models, we desire to get a sense as to how the different approaches performed. For each model, our optimization produces estimates of 78 moguls (right & left tracks for 39 moguls) for which we compute the RMS error. To gain insight into the performance of each model we then compute some basic statistics of these 78 measures. Table 1 shows these results for the minimum, maximum and mean RMS errors.

Figure 9 shows pictorially how well our mogul approximations did. It is interesting to note that regardless of the chosen model, there are some moguls which fit remarkably well and that the worst case for each mogul model subjectively looks like a good fit as well. That is why we will now turn to vehicular response evaluation.

4 Vehicular Response Evaluation

We now turn our attention to the evaluation of the modeled mogul shapes from the point of view of a vehicle dynamics model. In this section we will evaluate each mogul model with respect to its affect on the response of an Army vehicle, specifically the HMMWV. For the original mogul and each of our five models we will generate a short profile and run the HMMWV dynamics model over the mogul at speeds varying between 8 kph (5 mph) and 48 kph (30 mph) at 8 kph (5 mph) intervals (only four of these speeds are reported in this paper). We will then examine measures from the dynamics model to assess the pitch/heave dynamics of the model under various representations of the same mogul. We begin with a description of the HMMWV model.

Table 1. Statistics of the RMS error for 39 moguls.

	Gauss	**Hann**	**SVM**	**2-Gauss**	**Ratio-Gauss**
min [cm]	0.87	1.31	1.24	***0.57***	0.61
max [cm]	2.43	3.13	***1.64***	2.05	2.11
mean [cm]	1.62	2.30	1.42	***1.10***	1.21

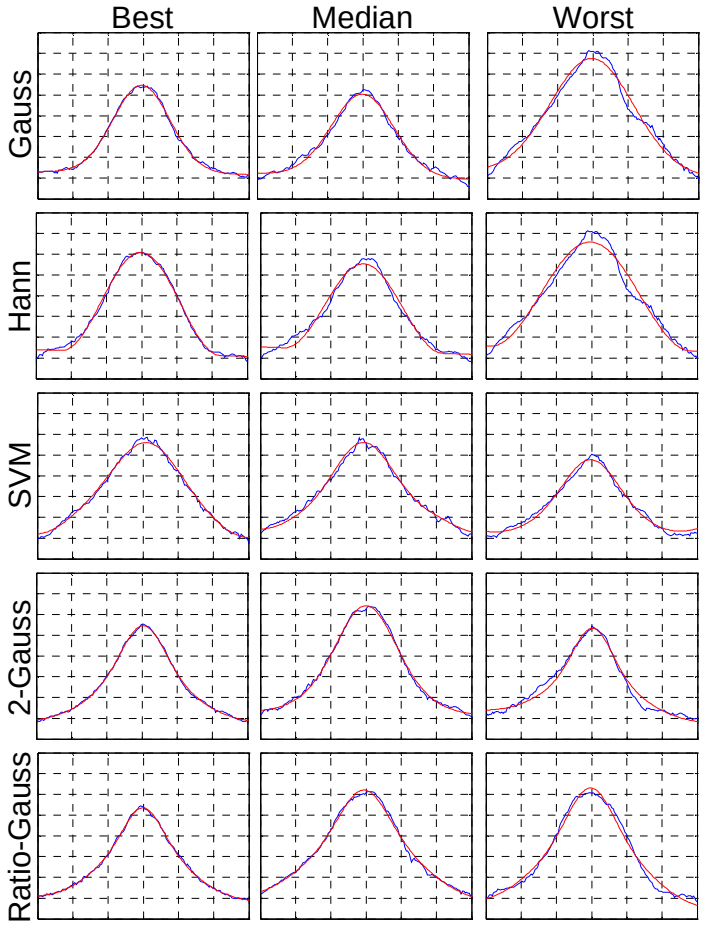

Figure 9. Pictorial representation of the fit of the five different mogul models. Shown in the rows are each of the five different modeling schemes and in the columns are the best, median and worst fit for each mogul model. Axes for all plots are [-6m, +6m] for the horizontal axis and [-0.1m, +0.7m] for the vertical axis.

4.1 Dynamics Model

The dynamics model is a rigid-body model of the M1114 High Mobility Multi-purpose Wheeled Vehicle (HMMWV). Figure 10 shows the exterior dimensions. The Gross Vehicle Weight (GVW) of 5,970 kg (13,160 lbs), consisting of 21 rigid bodies, includes a crew weight of 490 kg (1,080 lbs) and a 1,034 kg (2,280 lbs) payload. Tire pressures are set at 276/345 kPa (40/50 psi) for the front and rear tires, respectively.

The vehicle's tire model is based on a distributed contact method. The normal deflection and velocity are computed based upon the intersection of the undeformed tire circle and terrain profile. The tire circle is divided into vertical 'slices'. Once the total intersected area is found, an equivalent normal deflection is found by equating the intersected area with that for the tire on a flat surface, where the intersection would define a chord of the circle. The point of application for the tire force is found through a weighted average of the centroids of the partial intersected areas for each slice. Likewise, the direction of the force is found through a weighted average of the terrain normal vectors associated with the partial intersected areas of each slice. The tire

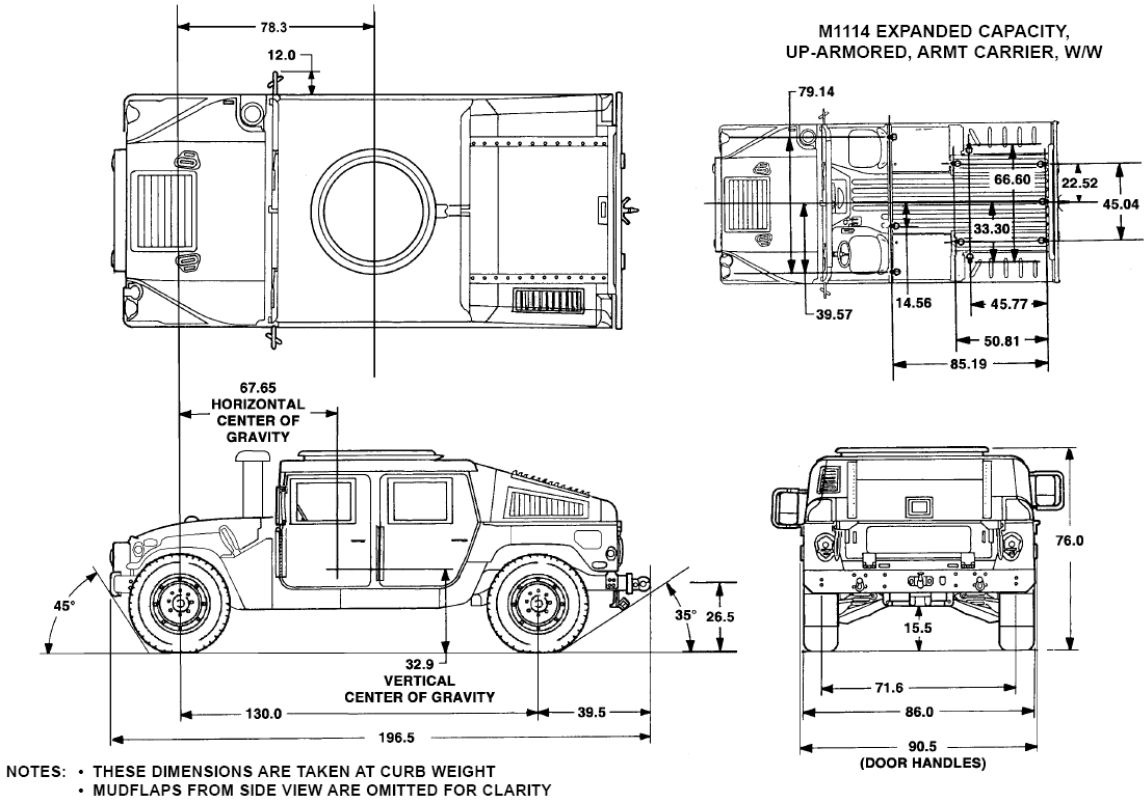

Figure 10. HMMWV Exterior Dimensions [inches].

model incorporates vertical force versus deflection curves, as provided by the manufacturer, including the nonlinear effect of contacting the run-flat.

The suspension model consists of four independent double "A" arm suspension units, one upper and lower control arm for each wheel. Each "A" arm is connected to the chassis by a revolute joint, which allows vertical rotation. The "A" arms are also connected to the wheel spindles by a spherical joint, which permits each wheel to rotate laterally and about the vertical axis. This combination allows each wheel to move vertically relative to the chassis and to rotate around a fore-aft or roll axis. Front tie-rods and rear radius rods, connected between the chassis frame and each wheel assembly, control the static toe-in angle, roll steer effect, and the wheel steer direction. The rear radius rods prevent the rear wheels from steering.

Vertical suspension forces are provided by four constant-rate coil springs with stiffness of 350 kN/m (2,000 lbs./in) in the front and 525 kN/m (3,000 lbs./in) in the rear and four telescoping translational shock absorbers (located inside the spring elements) represented by eight translational springs attached between the chassis and the lower "A" arms. Jounce and rebound travel is limited by these shock absorbers. The shocks provide a damping force proportional to the relative velocity between the shock piston rod and the shock piston cylinder. The shock has three ranges of operation; a midstroke region and two hydraulic bump stop regions (jounce and rebound). The hydraulic bump stops are built into the shocks near the end of travel in each direction to increase the damping force before metal to metal contact occurs.

The model was built in the Dynamic Analysis and Design System (DADS®) version 9.6 analysis tool. There were six variants of each of the 39 moguls to be run at 6 speeds resulting in 1,404

model runs in support of this analysis. For each run the DADS model generated 32 channels of data reported at a rate of 100 Hz. The channels reported include the linear position, velocity, and acceleration of the vehicle chassis, acceleration at the driver's position, the vehicle pitch and roll positions and velocities, the vehicle speed, the terrain elevation under each of the front wheels, the four suspension deflections, the four tire deflections and forces.

4.2 Results

In our analysis we compare the response generated by the mogul model $r_m(t)$ to the response generated by the actual mogul profile segment $r_p(t)$ by computing the error as $e(t) = r_m(t) - r_p(t)$ with the time t ranging from the time that the vehicle initially impacts the mogul to the time corresponding to 18.54 m (50 ft. + 130 in.) after impact. We reduce the error time history to a single statistic by computing its RMS value for selected channels and only report relative errors which are computed as $e_{\text{rel}} \triangleq \text{RMS}(e(t)) / \text{RMS}(r_p(t))$. Of the 32 channels reported by the dynamics model we will chose the driver's seat vertical acceleration, vehicle pitch angle, vehicle pitch angle rate, suspension deflection, tire deflection and tire force on which to compute error statistics. For the channels which are reported per wheel, we report the statistic taken over all four corners. These statistics are shown in Table 2. To clarity these results we have plotted the

Table 2. Statistics of the HMMWV model response for 39 moguls.

Speed/Channel		Gauss			Hann			SVM			2-Gauss			Ratio-Gauss		
		min	max	avg	min	max	avg	min	max	avg	min	max	avg	min	max	avg
16.1 kph (10 mph)	Driver's zdd	56.6	94.7	80.7	67.9	125.2	113.3	48.6	82.0	63.5	23.3	76.0	44.8	24.6	139.6	53.0
	Pitch	5.0	16.6	12.3	9.7	23.6	18.5	8.0	13.5	10.4	2.1	14.3	6.7	2.1	14.6	7.5
	Pitch rate	11.1	32.8	23.5	16.6	49.0	34.1	14.9	27.0	19.7	5.4	24.1	12.9	6.4	25.6	14.9
	Avg Susp Defl	42.7	53.6	48.7	60.2	79.3	70.4	33.3	41.0	37.9	23.3	26.1	25.0	26.8	31.5	29.8
	Avg Tire Defl	8.2	9.1	8.6	11.0	12.7	11.8	6.9	7.1	7.0	4.5	5.6	5.0	5.4	6.3	5.8
	Avg Tire Force	10.4	10.6	10.5	13.6	14.8	14.2	8.4	9.2	8.8	5.7	7.6	6.6	6.7	8.3	7.5
24.1 kph (15 mph)	Driver's zdd	37.9	87.7	62.3	63.7	111.7	97.9	31.8	66.8	47.7	17.0	65.8	32.2	18.6	96.9	36.8
	Pitch	4.3	15.3	11.1	9.0	23.1	17.1	6.9	12.4	9.5	1.5	14.6	6.5	2.2	17.3	7.3
	Pitch rate	6.4	29.2	18.2	12.4	44.3	27.7	8.5	23.0	14.7	3.0	20.9	10.2	4.4	21.0	11.7
	Avg Susp Defl	37.6	43.2	40.1	59.0	64.5	61.3	27.5	32.6	29.7	18.3	20.2	18.9	21.0	24.2	22.3
	Avg Tire Defl	12.1	15.3	13.8	19.1	22.1	20.6	9.3	12.4	10.8	6.3	8.1	7.1	7.2	9.3	8.3
	Avg Tire Force	13.7	17.4	15.6	21.8	25.3	23.5	10.7	14.2	12.4	7.8	10.4	9.1	8.7	11.6	10.2
32.2 kph (20 mph)	Driver's zdd	21.6	66.8	44.7	35.4	82.7	64.2	24.9	49.6	36.5	16.2	59.8	28.4	18.8	63.3	31.3
	Pitch	5.1	20.0	13.2	12.3	30.3	20.4	8.2	14.8	11.6	1.7	21.5	6.5	1.2	24.1	7.8
	Pitch rate	7.6	28.2	18.9	16.6	42.4	29.0	11.0	20.2	14.8	2.5	25.7	9.0	2.5	29.4	10.8
	Avg Susp Defl	26.5	29.2	27.8	39.1	43.9	41.5	20.0	22.5	21.2	13.3	15.0	14.0	15.5	17.7	16.5
	Avg Tire Defl	12.1	15.6	13.8	18.3	23.0	20.6	9.7	13.3	11.5	7.2	8.6	7.9	8.0	10.2	9.1
	Avg Tire Force	15.0	18.4	16.6	21.9	26.4	24.0	11.6	15.8	13.7	9.4	11.4	10.4	10.4	13.1	11.7
40.2 kph (25 mph)	Driver's zdd	22.9	61.3	38.1	18.5	75.1	52.8	19.9	64.8	40.0	9.2	68.9	26.9	9.5	74.7	28.2
	Pitch	3.9	21.0	10.8	4.8	27.8	16.9	3.3	21.8	12.0	1.0	29.7	7.6	1.7	32.0	7.7
	Pitch rate	5.8	26.0	15.1	6.8	38.4	23.5	5.2	29.0	16.1	1.6	36.6	9.7	2.5	39.3	10.2
	Avg Susp Defl	19.3	24.9	22.1	29.1	37.4	33.1	17.9	23.8	20.8	13.5	13.8	13.6	13.8	15.6	14.6
	Avg Tire Defl	11.9	18.2	15.0	17.5	26.9	21.8	13.0	20.0	16.0	10.1	11.4	10.8	9.7	12.4	11.2
	Avg Tire Force	14.9	22.2	18.4	22.0	32.0	26.5	17.1	24.6	20.1	12.8	14.2	13.7	12.3	15.5	14.1

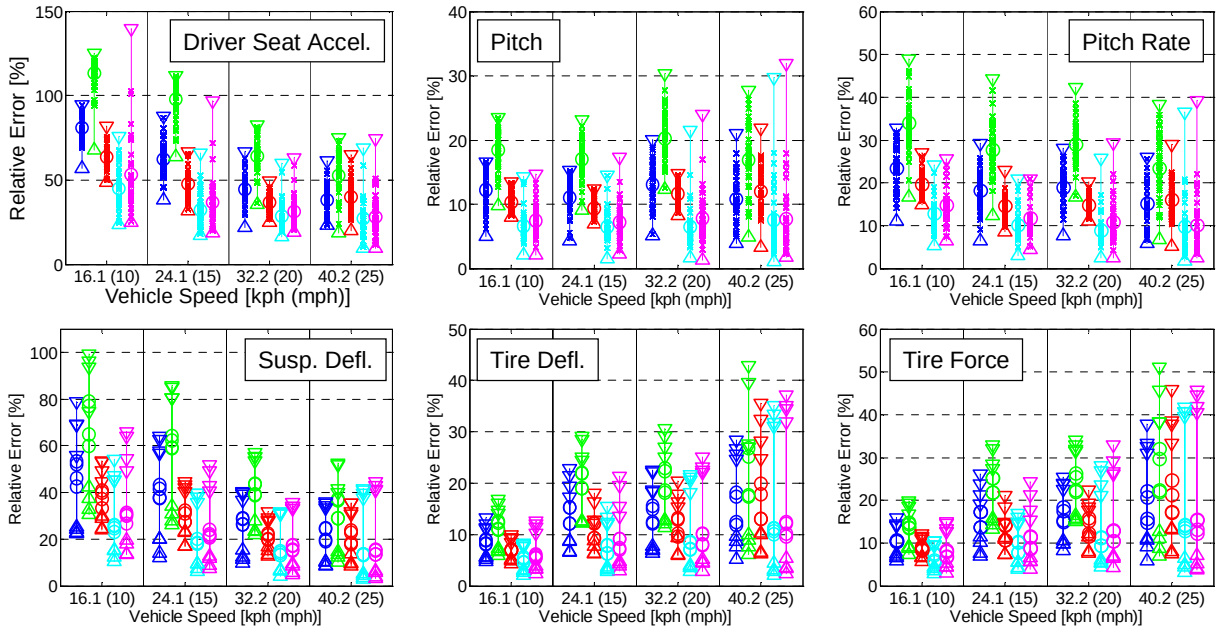

Figure 11. Plots showing the relative errors vs. speed for each of the five mogul models. The plots show the driver's vertical acceleration, pitch, pitch rate, suspension deflection, tire deflection and tire force respectively. The △, ▽, and ○ symbols represent the minimum, maximum and mean respectively. The × symbol shows individual relative errors for each of the moguls. The bottom three plots are shown for each of the four corners. For each speed the mogul models from left to right are the Gaussian, Hanning Window, SVM, 2-Gaussian and ratio-Gaussian. Note that plots are at different scales.

same statistics in Figure 11. There we observe that typically the best performer is the two-Gaussian model followed closely by the ratio-Gaussian model, the next best model appears to be the SVM followed by the Gaussian model. The worst performer is the Hanning window. We may also examine Figure 11 from the perspective of speed. It appears that for the vehicle sprung mass there appears to be a negligible to slight improvement in the relative error with increasing speed. On the other hand for the tire deflection and force, there is a slight increasing trend with vehicle speed. The worst performing channel is the driver's vertical acceleration. We suggest that this is the case because of the roughness in the original profile which is not present in the mogul model. Acceleration signals are particularly sensitive to the high-frequency nature of the roughness and thus the relative roughness/smoothness is highlighted in acceleration signals.

Since the two-Gaussian and ratio-Gaussian models perform similarly it is reasonable to ask: which is the better model? Although the two-Gaussian function performs slightly better, it does not define a shape for the prototypical mogul due to its mathematical structure. Our desire is to obtain a prototypical shape which may be parameterized by width and amplitude. In this case we choose the ratio-Gauss function to be the best representation of the 39 moguls that we have examined. Given this conclusion, we illustrate (in Figure 12) the performance of this model for the median performer, mogul number 39. There we observe time histories of the channels used in this study. By observing the driver's vertical acceleration, it is evident that the high-frequency components of the signal are largely contributing to the error. Some of this high frequency

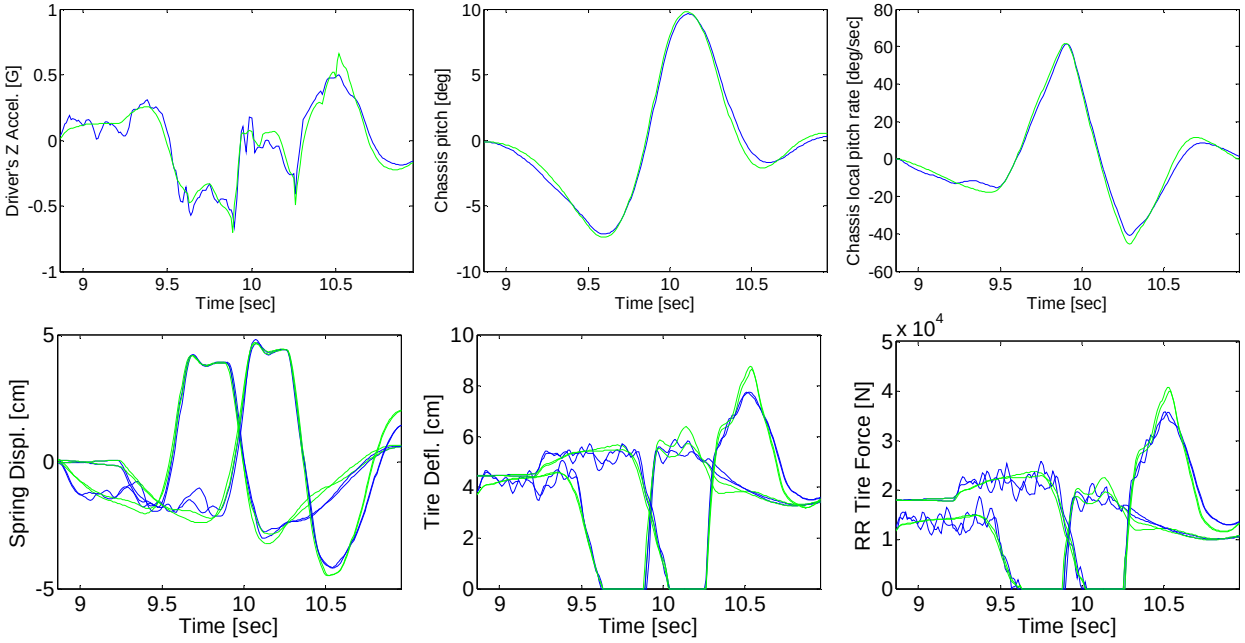

Figure 12. Plots showing the reference (blue) and the model (green) responses for the ratio-Gauss mogul at 32.2 kph (20 mph), shown are responses from mogul 39 which represents the responses whose error are closest to the median error.

behavior may be observed in the tire deflection and forces as well. We should note that at higher speeds, the shape of the mogul dominates the vehicle response, while at the lower speeds, the surface roughness tends to dominate the response. Although the responses shown in Figure 12 subjectively appear to be very good, they would be worse at the slower speeds.

5 Conclusion

In this paper we have discussed modeling the shape of discrete features on an Army endurance test course. We illustrated why existing statistical techniques are not well suited for characterizing and synthesizing these features. We offer five functions as candidates with which to model the shape of the moguls. These shape functions varied in the number of free parameters available. The Gaussian and the Hanning window shapes were parameterized by width and amplitude, the SVM function technically has 161 free parameters, although most vanish in the optimization. The two-Gaussian function has four free parameters and the ratio-Gauss has two free parameters. We evaluated the quality of each model by computing the RMS elevation error of each fit and by examining the dynamic response of a HMMWV model. For the HMMWV model we examined six different types of signals related to the chassis, suspension and tires. We evaluated the quality of the mogul model by again computing the RMS error over each reference signal for four different speeds. After examining the response errors, we concluded that the two-Gaussian and ratio-Gaussian functions give the best approximation of the moguls. Among these two functions we conclude that the ratio-Gauss function is preferred because it has fewer free parameters and has a definite shape. We therefore conclude that the 39 moguls on this test course are best modeled by (7) and (8) with $p_\sigma = 0.431$, $p_a = 0.551$ and the distribution of width and amplitude given by the distribution shown in Figure 8.

The analysis in this paper was conducted for the profile as measured in 2002. This profile has been periodically surveyed by the Army's profilometer for a decade. Future work may include an analysis of how these moguls change over time. Also, there are other potential candidate functions which were not evaluated in this study. Future work may include the evaluation of functions such as $\mathrm{sech}(\cdot)$ and $\frac{d}{dx}\tanh(x) = 1 - \tanh^2(x)$.

References

Castaldo, P.D., Allred, J.A., Reil, M.J. c. 1991. "Terrain Profilometer", Unpublished, Aberdeen Proving Ground, Aberdeen, MD.

Cristianini, N., Shawe-Taylor, J. 2000. An Introduction to Support Vector Machines, Cambridge University Press, New York, NY.

Ferris, J.B. "Characterising road profiles as Markov Chains". 2004. I*nternational Journal of Vehicle Design,* Vol. 36, No.2/3, pp. 103 - 115.

Frinkle, M., Ferris, J.B., Weir, R.P. 2004. "A Graphical Representation of Road Profile Characteristics", 2004-01-0769, Society of Automotive Engineers, Warrendale, PA.

Gorsich, D.J., Gunter, D.D., Karlsen, R., Chaika, M. 2003. "Terrain Roughness Standards for Mobility and Ultra-Reliability Prediction", Paper 2003-01-0218, Society of Automotive Engineers.

Grinstead, B., Koschan, A.F., Page, D., Gribok, A., Abidi, M.A. 2005. "Vehicle-Borne Scanning for Detailed 3d Terrain Model Generation", Paper 2005-01-3557, Society of Automotive Engineers, Warrendale, PA.

Howe, J.G., Lee, D.C., Chrstos, J.P., Balling, O., Myers, T.T., Allen, R.W., Gorsich, D.J., Reid, A.A. 2005. "Further Analysis of Potential Road/Terrain Characterization Rating Metrics", 2005-01-3562. Society of Automotive Engineers, Warrendale, PA.

Howe, J.G., Lee, D.C., Chrstos, J.P., Myers, T.T., Allen, R.W., Reid, A.A., Gorsich, D.J. 2004. "Analysis of Potential Road/Characterization Rating Metrics", Paper 2004-01-2640. Society of Automotive Engineers, Warrendale, PA.

Morrison, M.M., Romano, R.A., Reid, A.A., Gorsich, D.J. 2004. "High-Frequency Terrain Content and Surface Interactions for Off-Road Simulations", Paper 2004-01-2641. Society of Automotive Engineers, Warrendale, PA.

Lin, J. and Kanellakopoulos, I. 1995. "Nonlinear Design of Active Suspensions", Proceedings of the 34th IEEE Conference on Decision and Control, New Orleans, LA, pp. 3567-3569.

Sandu, C., Sandu, A., and Li, L. 2005. "Stochastic Modeling of Terrain Profiles and Soil Parameters", Paper No. 2005-01-3559, Society of Automotive Engineers, Warrendale, PA.

Sandu, C., Li, L. 2007. "Modeling and Simulation of 2D ARMA Terrain Models for Vehicle Dynamics Applications", 2007. Paper 2007-01-0138, Society of Automotive Engineers, Warrendale, PA.

Sayers, M. W. and Karamihas, S. M. *Interpretation of Road Roughness Profile Data – Final Report*. 1996. Report UMTRI 96-19, University of Michigan, Transportation Research Institute, Ann Arbor, MI.

Sayers, M. W. and Karamihas, S. M. *The Little Book of Profiling: Basic Information About Measuring and Interpreting Road Profiles*. 1998. University of Michigan, Transportation Research Institute, Ann Arbor, MI.

Special Issue on Road Profiles: Measurement, Analysis, and Applications. Ferris, J.B., editor. 2004. *International Journal of Vehicle Design,* Vol. 36, No.2/3.

Steinwolf, A., Connon, W.H. III. 2005. "Limitations of the Fourier Transform for Describing Test Course Profiles", *Sound and Vibration Magazine*, Vol. 39(2), February 2005.

Sun, T.C., Gorsich, D., Chaika, M., Alyass, K., Wei, J., Ferris, J. "Time Series Modeling of Terrain Profiles", Paper 2005-01-3561. Society of Automotive Engineers, Warrendale, PA.

Tikhonov, A.N., Arsenin, V.Y. 1977. Solutions of Ill-Posed Problems. V.H. Winston & Sons, Washington D.C. English translation by Fritz John.